웨이블릿 변환과 보간법을 이용한 OFDM 파일럿 지원 채널 추정기술

공 형 윤[†] · Ho Van Khuong[††] · 남 두 희[†††]

요 약

본 논문에서는 웨이블릿 변환과 보간법을 이용하여 OFDM(Orthogonal Frequency Division Multiplexing)시스템을 위한 새로운 파일럿 지원 채널 추정 기법을 소개한다. 웨이블릿 변환의 AWGN(Additive White Gaussian Noise) 감쇄능력이 뛰어남으로 인해 파일럿 채널은 아주 정확하게 추정될 수 있고, 이렇게 추정된 파일럿 데이터는 남아있는 다른 데이터 심볼 채널에 대해 2차 다항식 보간법을 하는데 사용된다. Short WATM(Wireless Asynchronous Transfer Mode)채널에 대한 모의실험 결과를 통해, 이 추정기를 쓴 OFDM 시스템의 성능은 완벽한 CSI(Channel State Information)에서 발생하는 BER(Bit Error Ratio) 성능과 거의 비슷한 것을 확인할 수 있다.

키워드 : 주파수 분할 다중접속, 웨이블릿 변환, 채널추정, MMSE

Pilot-Aided Channel Estimation for OFDM System Using Wavelet Transform and Interpolation

Hyung-Yun Kong[†] · Ho Van Khuong[††] · Doo-Hee Nam[†††]

ABSTRACT

We present a novel pilot-aided channel estimation method for OFDM (Orthogonal Frequency Division Multiplexing) system using WT (Wavelet transform) and interpolation. Due to excellent AWGN (Additive White Gaussian Noise) cancellation capability of WT, pilot channels are estimated quite exactly and then, they are used in 2-degree polynomial interpolating the other remaining data symbol channels. The simulation results for Short WATM (Wireless Asynchronous Transfer Mode) channel show that the degradation in BER (Bit Error Ratio) performance of OFDM system with this estimator is negligible compared to the case of perfect knowledge of CSI (Channel State Information).

Key Words : OFDM, Wavelet Transform, Channel Estimation, MMSE

1. Introduction

Communication channel makes signal pulses broadened in time as they travel through the channel (multi-path effect), leading to Inter-Symbol Interference (ISI). The pulse spread restricts the speed at which adjacent data pulses can be sent without overlap, thus limiting the maximum information rate of the wireless system. One technique to avoid the detrimental effect of multi-path, without sacrificing the transmission rate, is OFDM (Orthogonal Frequency Division Multiplexing) modulation [1]. This is a parallel transmission scheme, where the overall frequency band is divided into a number of subbands with separate subcarriers. On each subcarrier, the modulated symbol rate is low in comparison to the channel delay spread, thus ISI can be prevented. Moreover, by such subdivision, each subband suffers a flat-fading and hence, OFDM is robust against the frequency selective fading. However, in order to support the coherent detection techniques at the receiver in obtaining their fullest abilities, channel estimator has to work efficiently to provide CSI (Channel State Information).

The term "Wavelet" was first mentioned in Alfred Haar's thesis in 1909. Since then, it has been attracted the interest of signal processing researchers. Due to WT capable of flexibly analyzing the signal in both time and frequency

※ 본 연구는 정보통신부 및 정보통신연구진흥원의 대학 IT 연구센터 육성지원사업의 연구결과로 수행되었습니다.
† 정 회 원 : 울산대학교 전기전자정보시스템공학부 부교수
†† 준 회 원 : 울산대학교 전기전자정보시스템공학과 박사과정
††† 준 회 원 : 울산대학교 전기전자정보시스템공학과 석사과정
논문접수 : 2005년 4월 6일, 심사완료 : 2005년 7월 4일

(scale) dimensions by choosing the appropriate shift and scale factors, it has been applied popularly in many fields for recent years, especially, in noise suppression [2]-[6] and signal compression. In this paper, we take advantage of WT in quite completely suppressing AWGN (Additive Gaussian White Noise) to estimate pilot channel coefficients which are used to 2-degree polynomial interpolate other data channels.

2. OFDM System

A discrete-time base-band model of OFDM system with channel estimator is shown in (Fig. 1). A data block of B modulated symbols is serial-to-parallel converted and multiplexed with P equidistantly interleaved pilots to generate $d(n)$, $n=1,\cdots,N$ in which $N=P+B$ is the number of subcarriers. In OFDM system, the multicarrier modulation is implemented by N-point IDFT computation on the signal $d(n)$ and the result of this operation is the following signal:

$$S(m)=IDFT[d(n)]=\frac{1}{N}\sum_{n=1}^{N}d(n)e^{j2\pi nm/N},\ \mathrm{m}=1,..,\mathrm{N} \quad (1)$$

The signal then is transmitted through the channel with the impulse response $h(k)$, $k=0,\cdots,K-1$ and corrupted by Gaussian noise. Therefore, the received signal is given by:

$$R(m)=S(m)*h(m)+g(m) \quad (2)$$

where $*$ is convolution operator and $g(m)$ is Gaussian noise.

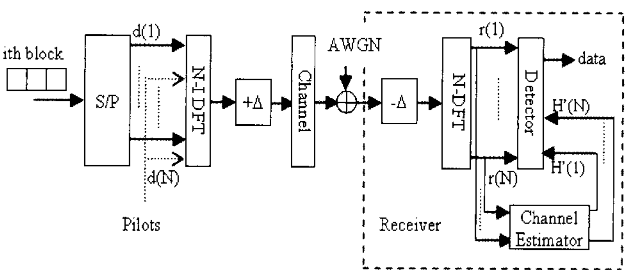

(Fig. 1) OFDM System Model

To recover the transmitted symbols, the receiver computes N-point DFT on the signal $R(m)$. Assume that the phase and frequency synchronization is perfect and the guard interval Δ is large enough to completely suppress ISI, the generated signal after DFT block is:

$$r(n)=DFT[R(m)]=d(n)H(n)+G(n),\ \mathrm{n}=1,...,\mathrm{N} \quad (3)$$

where $H(n)$ and $G(n)$ are DFTs of $h(m)$ and $g(m)$, respectively; $G(n)$ is an i.i.d Gaussian noise with zero-mean and variance σ^2.

The data detection for $d(n)$ can be performed by finding equalization coefficients $w(n)$ that reduces the effect of fading at most. Based on MMSE (Minimum Mean Square Error) condition, $w(n)$ are found by minimizing the cost function

$$E\{|d(n)-w(n)r(n)|^2\} \quad (4)$$

Here $E\{\cdot\}$ is the expectation operator.

The above optimal problem is easily solved with the solution as

$$w(n)=\frac{H^*(n)}{|H(n)|^2+\sigma^2/E\{|d(n)|^2\}} \quad (5)$$

As usual, $H(n)$ is unknown at the receiver and it can be obtained by the channel estimator as $H'(n)$. Then, the restored data is given by $d'(n)=w(n)r(n)$.

2.1 Channel Model

The complex equivalent low-pass time-variant impulse response of p-path frequency selective Rayleigh fading channel is given by [7]

$$h(t,\tau)=\sum_{i=1}^{P}g_i(t)\delta(t-\tau_i) \quad (6)$$

where $g_i(t)$, τ_i are gain and delay of the i^{th} path in the power delay profile of channel. This paper assumes the channel to be WSSUS (Wide Sense Stationary Uncorrelated Scattering), and thus, $g_i(t)$ is a mutually independent complex Gaussian random process with zero mean, variance σ_{gi}^2 (Jakes-like algorithm for $g_i(t)$ coefficients generation found in [7]) and the autocorrelation function [7]:

$$R_{gi}(\Delta t)=\sigma_{gi}^2.J_0(2\pi f_{d\max}\Delta t) \quad (7)$$

in which $J_0(\cdot)$ and f_{dmax} are the zero-order Bessel function of the first kind and maximum Doppler frequency, res- pectively.

If the condition $\Delta f \ll B_C \ll BW$ (Δf: frequency distance between two adjacent carriers, B_C: coherent bandwidth of channel, BW: total bandwidth of system) is satisfied, then each subcarrier only undergoes a flat fading. Therefore, the Fourier transform of $h(t,\tau)$ is the channel's frequency domain transfer function $H(n)$ of the following form:

$$H(n) = \alpha_n e^{j\phi_n} \quad (8)$$

where α_n is the amplitude and ϕ_n the phase in the n^{th} subchannel or the n^{th} subcarrier due to fade; α_n, ϕ_n are unchanged during each symbol interval but fluctuate over longer periods of time.

3. Wavelet Transform

The continuous WT of a signal $f(t) \in L_2(R)$ is defined as [8].

$$CWT(a,b) = \int_{-\infty}^{\infty} \psi^{*}_{a,b}(t) f(t) dt = \langle \psi_{a,b}(t), f(t) \rangle \quad (9)$$

where < · > is the inner product and $\psi_{a,b}(t)$ is a function obtained by shifting and scaling a "mother wavelet" $\psi(t) \in L_2(R)$,

$$\psi_{a,b}(t) = \frac{1}{\sqrt{|a|}} \psi\left(\frac{t-b}{a}\right) \quad (10)$$

where a, b ∈ R (a ≠ 0), and the normalization ensures that $\|\psi_{a,b}(t)\| = \|\psi(t)\|$.

Moreover, the wavelet satisfies the admissibility condition where $\Psi(w)$ is the Fourier transform of $\psi(t)$.

$$\int_{-\infty}^{\infty} \frac{|\Psi(\omega)|^2}{|\omega|} d\omega < \infty \quad (11)$$

Wavelet-transforming a signal for every continuous scale and shift by using Eq. (9) is time-consuming and requires a huge memory volume to store the result. To alleviate these wastes, Mallat produced a fast wavelet decomposition and reconstruction algorithm known as a two channel subband coder using conjugate quadrature filters [9].

Let *a(n)* be the noise-free signal and *f(n)* the signal corrupted with white noise *g(n)*, i.e., $f(n)=a(n)+\sigma g(n)$, where *g(n)* has a normal distribution *N(0,1)* and σ is noise level. Since WT is able to concentrate signal energy on a few of the wavelet coefficients and white-noising is still white-noising at any orthogonal base transform and possesses the same value, the value of signal wavelet coefficient must be larger than the value of nosing wavelet coefficient whose energies are dispersed and its amplitudes are small. We can obtain the aim of denosing and keeping the useful signal with selecting a proper threshold and handling wavelet coefficient with thresholds and finally, performing the inverse wavelet transform. For the more detailed explanation on the optimal threshold for each wavelet decomposition level, the reader is referred to [10], [11], [12] in which "heursure" soft-thresholding method takes advantage of universal threshold and the other based on the use of Stein's Unbiased Risk Estimate [11]. For selecting wavelet basis, [13] shows that in practice it is not possible to determine the optimal wavelet basis for a given signal. Some attempts to an estimate of the optimal basis have been proposed in [14]. Finally, the number of Wavelet decomposition levels is the trade-off between the signal resolution in Wavelet domain and processing time.

From the above analysis, this paper chooses the parameters for WT-based de-nosing :

- Wavelet family "sym8" [12] for its symmetry and short length with the time-domain waveform W(n) = {0.0013, -0.0002, -0.0106, 0.0027, 0.0347, -0.0192, -0.0367, 0.2577, 0.5496, 0.3404, -0.0433, -0.1013, 0.0054, 0.0224, -0.0004, -0.0024}. From W, we create filters LoF_R = W/norm (W), LoF_D = rev(LoF_R), HiF_R = qmf (LoF_R), HiF_D = rev(HiF_R) in which qmf(·) is such that HiF_R and LoF_R are quadrature mirror filters (i.e., $HiF\_R(k)=(-1)^k\, LoF\_R(2N-1-k)$); rev(·) flips the filter coefficients and norm(·) is normalization operator.
- Mallat algorithm for 3-level Wavelet decomposition and reconstruction. First, *f(n)* is decomposed into two sets : approximation coefficients cA_1 and detail coefficients cD_1. These sets are obtained by convolving f(n) with LoF_D for approximation F, and with HiF_D for detail G. Then F and G are downsampled by factor 2 as in (Fig. 2a). For high-level Wavelet decomposition, the above procedure is repeated for the approximation coefficients cA_j until the expected level is reached.
- Adopt soft-thresholding with "heursure" rule

$$C'_j = \begin{cases} sgn(C_j)(|C_j| - \alpha), & |C_j| \geq \alpha \\ 0, & |C_j| < \alpha \end{cases} \quad (12)$$

where C_j and C_j' are the wavelet decomposition coefficients before and after thresholding at level j; α is threshold calculated by "heursure" rule [12]; sgn(·) is signum function.

Based on C_j', signal reconstruction is performed in the reverse order of (Fig. 2a). Starting from cA_j and cD_j (level-j), the Inverse-WT reconstructs cA_{j-1} by inserting zeros and convolving the results with the reconstruction filters (see (Fig. 2b)).

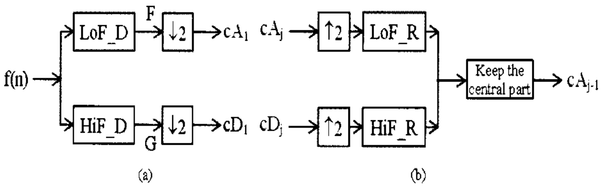

(Fig. 2) Mallat algorithm(↓ : downsampling, ↑ : upsampling)

4. Proposed Channel Estimation Algorithm

We deduce from Eq. (3) that if *d(n)* has a fixed value, then *r(n)* is the channel frequency response *H(n)* disturbed by the Gaussian noise. Therefore, by removing Gaussian noise component in the composite signal *r(n)*, we can obtain the CSI. In the aspect of AWGN suppression, it is obvious that WT is an appropriate choice. As a result, we suggest the channel estimation algorithm using pilot insertion and WT.

First, the same-value pilot symbols are inserted equidistantly into proper locations in frequency domain, where distance *Df* between two adjacent pilot symbols in terms of the number of sub-carriers obeys the sampling theorem [15]:

$$Df \le \frac{N}{2\tau_{\max}/T_s} \tag{13}$$

in which $\tau_{\max}$: maximum delay spread of channel; T_s: sampling period of the signal.

Next, estimating pilot channel gains and interpolating the remaining symbol channels are performed.

[16] used the LS (Least Square) condition to estimate pilot channel gains

$$H'_{LS}(p) = \frac{r(p)}{d(p)} = H(p) + \frac{G(p)}{d(p)} \tag{14}$$

where *d(p)* are pilot symbols having constant values and known at the receiver in advance; *r(p)*, *G(p)* are the received signal and Gaussian noise derived from (3), correspondingly and *p* the pilot position.

Based on Eq. (14), the above estimation causes severe error due to the term *G(p)/d(p)*. Because pilot symbols are used to interpolate the remaining data symbols, the inaccuracy of pilot estimation adversely affects on the overall result of estimation. As a result, in order to improve the reliability of estimator, [17] suggested MMSE estimator and thus leading to pilot channel gains given by

$$H'_{MMSE} = R_{fp}\left(R_{fp} + \frac{E\{|r(p)|^2\}}{SNR} I\right)^{-1} H'_{LS} \tag{15}$$

where I is an identity matrix; $R_{fp} \approx E\{H'_{LS} H'^{H}_{LS}\}$ denotes frequency domain correlation matrix; $E\{\cdot\}$, $[\cdot]^T$ and $[\cdot]^H$ are expectation, transposition and complex conjugate transposition operators; SNR is the signal to noise ratio; H'_{MMSE} and H'_{LS} are column-vectors whose elements are prdicted-pilot channel gains.

Although the MMSE estimator outperforms the LS estimator, it still suffers the problems of complicated matrix manipulation, frequency domain correlation matrix estimation as well as low efficiency. Therefore, we approach a novel technique using WT to suppress Gaussian noise *G(p)* in Eq. (3) as discussed in part 3. First of all, the real and imaginary parts of the vector $r=[r(1), r(2), \cdots, r(P)]^T$ at pilot positions are noise-removed separately before estimating pilot channels. (Fig. 4) shows the frequency response of channel with CIR in (Fig. 3) and the received signal corrupted by noise. Moreover, (Figs. 5c-d) is the result of WT-based noise cancellation for only received pilot signal *r(n)* of (Figs. 5a-b). Obviously, the denosing efficiency of WT is very high.

After noise-removing process, the resulting vector $r' = [r'(1), r'(2), \cdots, r'(P)]^T$ can be considered as the channel frequency response *H(p)* amplified by a constant factor *d(p)*. Therefore, pilot channel coefficients are identified as

$$H'(p) = \frac{r'(p)}{d(p)} \tag{16}$$

Once estimation of pilot channels is completed, the (*N-P*) remaining data symbols are interpolated by the equation:

$$H_{est}(p) = a.p^2 + b.p + c = [p^2 \;\; p \;\; 1][a \;\; b \;\; c]^T \tag{17}$$

where *p* is the position of subcarrier lying between three consecutive pilot symbols p_1, p_2, p_3 and the constants *a, b, c* are calculated with the aid of these three symbols as follows

$$\mathbf{H}_{est} = \begin{bmatrix} H'(p_1) \\ H'(p_2) \\ H'(p_3) \end{bmatrix} = \begin{bmatrix} p_1^2 & p_1 & 1 \\ p_2^2 & p_2 & 1 \\ p_3^2 & p_3 & 1 \end{bmatrix} \begin{bmatrix} a \\ b \\ c \end{bmatrix} = \mathbf{F}.\mathbf{Coef} \tag{18}$$

Therefore, **Coef** = $[a \;\; b \;\; c]^T = \mathbf{F}^{-1}\mathbf{H}_{est}$. The result of interpolation for the channel frequency response in (Fig. 3) is demonstrated in (Figs. 5e-f). When comparing these waveforms with those in (Figs. 4a-b), we realize that there is no significant difference.

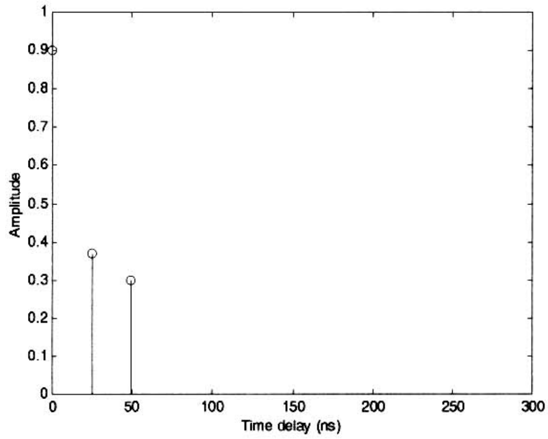

(Fig. 3) Channel impulse response (CIR) of Short WATM channel

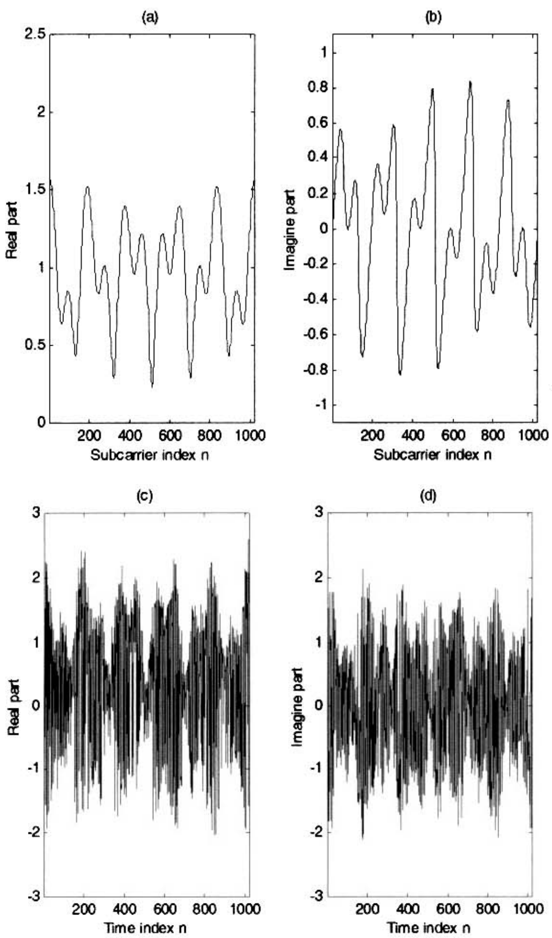

(Fig. 4) Frequency domain : (a) Real part of CIR in (Fig. 3), (b) Imaginary part of CIR in (Fig. 3), (c) Real part of the signal r(n), (d) Imaginary part of the signal r(n); SNR=15dB, spectrum of the signal is found by 1024-point DFT, QPSK-modulated data and pilot symbol of value $\sqrt{2}$, Df=3.

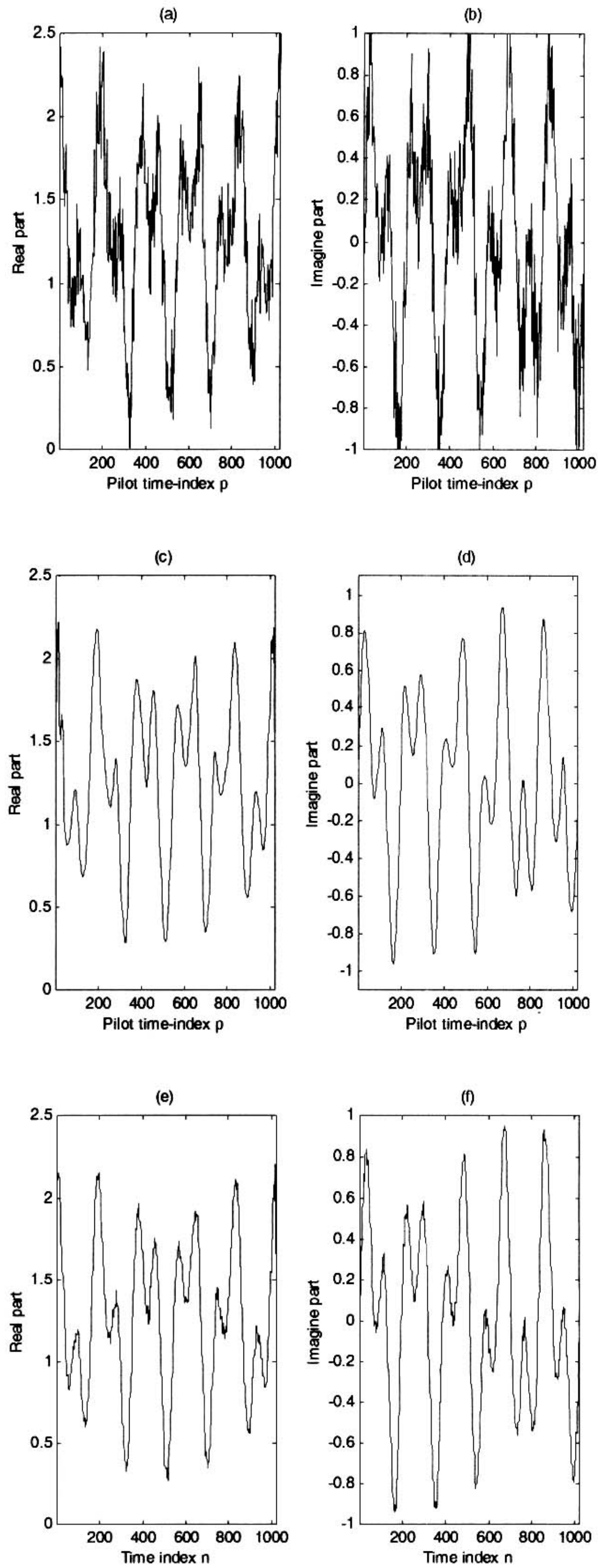

(Fig. 5) Frequency domain : (a) Real part of rp, (b) Imaginary part of rp, (c) Denoised real part of rp, (d) Denoised imaginary part of rp, (e) Estimated real part of H(n), (f) Estimated imaginary part of H(n); Df=3; rp : received pilot symbols vector in (Fig. 4)

5. Simulation results

The below presented simulation results assume that carrier and timing synchronization is perfect. The channel estimation performance is evaluated through the Mean Square Error (MSE) metric defined by

$$MSE = \frac{1}{N_s N}\sum_{j=1}^{N_s}\sum_{i=1}^{N}\left|H(i) - H_{est}(i)\right|^2 \tag{19}$$

where N_s are the investigated number of data blocks and $H(i)$, $H_{est}(i)$ are original and estimated sub-channel gains.

Short-WATM (Wireless Asynchronous Transfer Mode) channel [15] with maximal path delay τ_{max}=48.9 (ns) and RMS delay spread RMS(τ)=16.9 (ns) is examined. The other simulation parameters are N=1024, QPSK data modulation, sampling frequency $1/T_s$=225 Msamples/s and f_{dmax}=2778 Hz, 1000 data blocks used for calculating MSE for each SNR, pilot symbols with value of root square of 2 to have the same average power as data symbols. Moreover, WT-based denosing uses the parameters as mentioned in section 3. With these simulation parameters, the pilot symbol distance in Eq. (13) must be less than 46.6.

MSEs for different values of Df=3, 7, 11 are demonstrated in (Fig. 6). For any Df, the proposed algorithm dramatically improves the estimation performance over LS method with an average improvement in SNR of about 10dB for every SNR. In addition, the new method illustrates a better performance than the MMSE estimator with SNR gain of 4dB at MSE of 10^{-3} and Df=3. (Fig. 6) also shows that estimation performance is decreased as Df

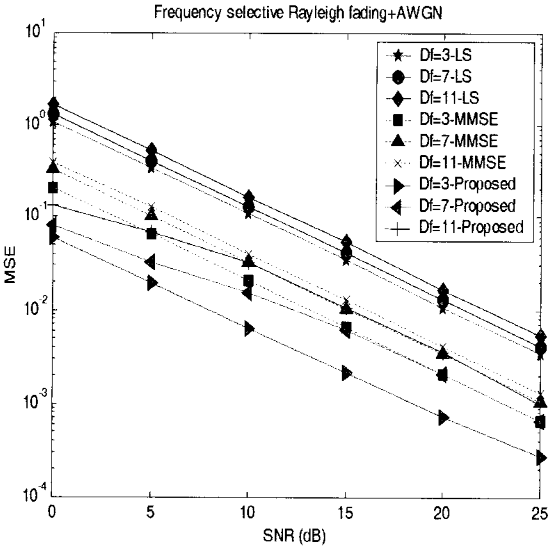

(Fig. 6) MSEs via different Dfs

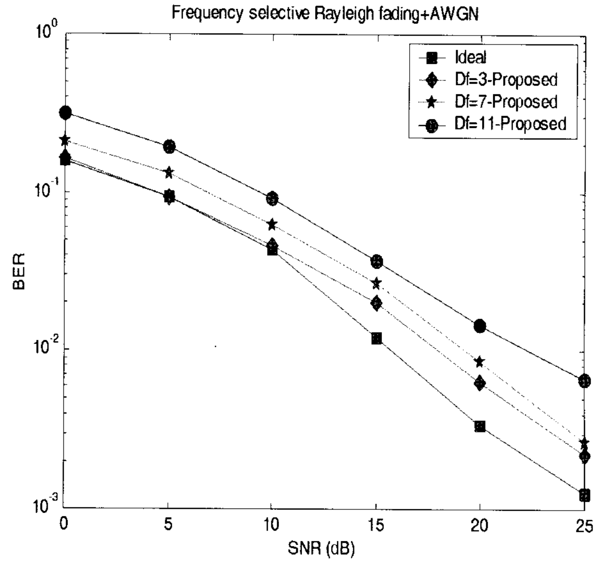

(Fig. 7) BER performance of OFDM system via Df

increases. It is logical because the increase in Df is equivalent to the performance deterioration of interpolation process.

As shown in (Fig. 7), BER performance of OFDM system with this estimator is significantly degraded according to the increase of Df. For example, at the target BER of 10^{-2} the difference in SNR of about 4dB between Df=3 and Df=11 can easily be recognized. However, as compared to the receiver with perfect CSI, the performance declination due to estimation error is only around 2.5dB at BER of 0.002 and Df=3. A trade-off between performance and bandwidth waste is also inferred. The smaller the Df, the better performance the system achieves.

6. Conclusion

Channel state information plays a crucial role in coherent detection of multi-carrier transmission systems. Recently, many channel estimation methods have been suggested, most of which focus on pilot-aided estimation. However, their drawback is to ignore the AWGN term and thus leading to the poor performance of estimator which has negative influence on the quality of system. Our algorithm overcomes this problem by applying WT. The simulation results for OFDM system over frequency-selective Rayleigh fading channel with AWGN demonstrate that the proposed estimator attains a greater 10dB SNR gain than least square method for every SNR and Df, and BER performance is decreased slightly as compared to that of the system with priorly known CSI. Moreover, the novel method shows better performance than MMSE estimator.

References

[1] Richard van Nee, Ramjee Prasad, "OFDM for Wireless Multimedia Communications", Artech House, 2000.

[2] A. L. Graps, "An introduction to wavelets", IEEE, Vol.2, p.50-61, Summer, 1995.

[3] Hyeokho Choi, Baraniuk R., "Multiple basis wavelet denoising using Besov projections", ICIP 99, Vol.1, p.595-599, 1999.

[4] Ranta R., Heinrich C., Louis-Dorr V., Wolf D., "Interpretation and improvement of an iterative wavelet-based denoising method", IEEE, Vol.10, pp.239-241, Aug., 2003.

[5] Chen, G.Y.; Bui, T.D., "Multiwavelets denoising using neighboring coefficients", IEEE, Vol.10, pp.211-214, July, 2003.

[6] Donoho, D.L., I.M. Johnstone, "Ideal de-noising in an orthonormal basis chosen from a library of bases'', CRAS Paris, pp.1317-1322, 1994.

[7] James K. Cavers, "Mobile Channel Characteristics", Kluwer Academic Publishers, 2000.

[8] Martin Vetterli, Jelena Kovacevic, "Wavelets and Subband Coding", Prentice Hall 1995.

[9] S. G. Mallat. "A theory for multiresolution signal decomposition: The wavelet representation", IEEE, Vol.11, pp.674-693, July, 1989.

[10] T.R. Downie and B. W. Silverman, "The discrete multiple wavelet transform and thresholding methods", IEEE, Vol.46, pp.2558-2561, Sept., 1998.

[11] Donoho D.L., "De-Noising by soft-thresholding", IEEE, Vol.41, pp.613-627, 1995.

[12] Michel Misiti, Yves Misiti, Georges Oppenheim, Jean-Michel Poggi, "Wavelet Toolbox User's Guide", The MathWorks, Inc., 1996.

[13] V. Bruni, D. Vitulano, "Signal Denosing via Overlapping Atoms in a Wavelet Domain", ISPA, Vol.1, pp.18-20, Sept., 2003.

[14] S. Mattlat, "Wavelet Tour of Signal Processing", Academic Press, 1998.

[15] L. Hanzo, M. Munster, B. J. Choi, T. Keller, "OFDM and MC-CDMA for Broadband Multi-User Commu- nications, WLANs and Broadcasting", John Wiley & Sons, Ltd, 2003.

[16] M. A. McKeown, D. G. M. Cruickshank, I. A. B. Lindsay, S. A. Farson and Y. Hu, "Pilot-assisted channel estimation in MC-CDMA for future mobile cellular systems", London Communications Symposium 2002.

[17] O. Edfors, M. Sandell, J.-J. van de Beek, S.K. Wilson, P.O. Borjesson, "OFDM channel estimation by singular value decomposition", IEEE Trans. Commu., Vol.46, Issue 7, pp.931-939, July, 1998.
Summary: We present and analyze low-rank channel estimators for orthogonal frequency-division multiplexing (OFDM) systems using the frequency correlation of the channel. Low-rank approximations based on the discrete Fourier transform (DFT) have been proposed,.....

[18] P. Marques, A. Gameriro, J. Fermandes, "Pilot-Aided Channel Estimation for MC-CDMA in Beyond 3G Wireless System", IST Mobile &Wireless Communications Summit 2003, Aveiro, 15-18 June, 2003.

공 형 윤

e-mail: hkong@mail.ulsan.ac.kr

1989년 미국 New York Institute of Technology 전자공학과(학사)

1991년 미국 Polytechnic University 전자공학과(석사)

1996년 미국 Polytechnic University 전자공학과(박사)

1996년~1996년 LG전자 PCS 팀장

1996년~1998년 LG전자 회장실 전략사업단

1998년~현재 울산대학교 전기전자정보시스템공학부 부교수

관심분야: 코딩(LDPC, Turbo) 및 모듈레이션 (OFDM, QAM), 멀티코드, Wireless Sensor Network 등

Ho Van Khuong

e-mail : khuongho2001@yahoo.com
2001년 베트남 HoChiMinh City University of Technology 전기전자공학과(학사)
2003년 베트남 HoChiMinh City University of Technology 전기전자공학과(석사)
2004년~현재 울산대학교 전기전자정보시스템공학과 박사과정
관심분야 : OFDM, MC-CDMA, 협력 통신, 채널 추정

남 두 희

e-mail : duheeya@mail.ulsan.ac.kr
2004년 울산대학교 전기전자정보시스템공학부(학사)
2004년~현재 울산대학교 전기전자정보시스템공학과 석사과정
관심분야 : LDPC, MC-CDMA, 멀티코드, 협력 통신, 센서 네트워크